ELSEVIER

Biochimica et Biophysica Acta 1280 (1996) 34–40

BBA Biochimica et Biophysica Acta

Time domain dielectric spectroscopy study of human cells. I. Erythrocytes and ghosts

Rosa Lisin [a], Ben Zion Ginzburg [b], Michael Schlesinger [c], Yuri Feldman [a,*]

[a] *School of Applied Sciences, The Hebrew University of Jerusalem, Jerusalem, Israel*
[b] *Plant Biophysical Laboratory, Institute of Life Sciences, The Hebrew University of Jerusalem, Jerusalem, Israel*
[c] *Hubert H. Humphrey Center of Experimental Medicine and Cancer Research, The Hebrew University, Hadassah Medical School, Jerusalem, Israel*

Received 31 May 1995; revised 11 October 1995; accepted 1 November 1995

Abstract

A method, allowing correction of electrode polarization effect in case of cell suspensions of small volume fraction is proposed. The dielectric behavior of human erythrocytes and erythrocyte ghosts suspensions was studied by time domain dielectric spectroscopy (TDDS) and the estimation of the dielectric constants of cell's structural parts (membrane, cytoplasm) on the basis of suitable models are presented. It was shown that in the case of small volume fraction of cells in suspension, the electrode polarization effect can be taken into account by the additional measurement of the corresponding supernatant. The optimal volume fraction of cells in suspensions in the TDDS measurements was found to be 3%–10%. The erythrocyte and erythrocyte ghost suspensions were found to demonstrate a single dispersion which can be described by the Debye equation. The membrane dielectric constant of different erythrocytes and ghosts was distributed near 5.

Keywords: Time domain dielectric spectroscopy; Dielectric constant; Erythrocyte; Erythrocyte ghost

1. Introduction

Analysis of dielectric properties of biological materials is of great importance for understanding of the structure and physical processes occurring in biological systems at different levels of complexity. Therefore, electrical measurements on living material are very significant in various areas of biophysics, physiology and medicine. Dielectric studies have provided a great deal of information on the structure and properties of biological molecules, cells and tissues which have not only biophysical and medical scientific significance, but also might have useful clinical applications [1–6].

One of the interesting subjects in biophysics is investigation of the dielectric properties of cells as a whole and of cell's structural parts (membrane, cytoplasm, etc.). These can provide valuable knowledge about different cell structures, their functions and metabolic mechanisms, which could hardly be obtained by other methods.

Before Time Domain Spectroscopy methods were developed, the investigations by Frequency Domain methods were restricted by lack of techniques which allowed quick determination of the dielectric spectrum within the frequency range 10^5–10^{10} Hz [1,2]. It was quite difficult to ensure the stability of biological materials because of the long duration of the experiment.

Time Domain Dielectric Spectroscopy (TDDS) [7–9] is based on measuring the response of the sample to a step-like signal, containing all the frequencies, instead of to a monochromatic signal in the above mentioned Frequency Domain technique. Thus TDDS allows to obtain information about dielectric properties in a wide frequency range during one measurement and hence to study unstable biologic systems properly. This is also a much less time-consuming method, which requires very few devices to work with. Moreover, the sensitivity of the system allows one to study dilute solutions or suspensions of cells (volume fraction < 10%).

One of the serious problems of the dielectric measurements of biologic materials is the high conductivity of the latter, which leads to the complex problem of electrode polarization. The methods of overcoming this problem were studied in frequency domain methods [1–3,10–12], but electrode polarization remains a big problem in time

* Corresponding author. Fax: +972 2 6528250. e-mail: yurif@vms.huji.ac.il.

SSDI 0005-2736(95)00266-9

domain measurements, where no general method accounting for it has been developed.

The purpose of the present work was to study ways of correction of the electrode polarization effect for cell suspension measurements, to investigate the dielectric behavior of erythrocyte and erythrocyte ghost suspensions by TDDS, and to estimate the dielectric constants of cell structural parts (membrane, cytoplasm) on the basis of suitable models.

2. Theory

2.1. Cell and cell suspension models

For analysis of the dielectric properties of suspensions of erythrocytes and erythrocyte ghosts several classical models are usually used [2,13–19]. For small volume fractions of cells the Maxwell-Wagner model is used, while for larger ones the Hanai formula would be preferable [2,16]. In our case (see Section 4.2) the dielectric spectra of a single cell were calculated from the Maxwell model of suspension [2], according to the mixture formula:

$$\epsilon^* = \epsilon_1^* \frac{(2\epsilon_1^* + \epsilon_2^*) - 2p(\epsilon_1^* - \epsilon_2^*)}{(2\epsilon_1^* + \epsilon_2^*) + p(\epsilon_1^* - \epsilon_2^*)} \quad (1)$$

where p is the cell's volume fraction.

$$\epsilon_1^*(\omega) = \epsilon_1 - i\frac{\sigma_1}{\epsilon_0 \omega}$$

is the complex dielectric permittivity of the suspending media, where ϵ_1 is its static permittivity and σ_1 is its conductivity; ϵ_2^* is the complex dielectric permittivity of cell. The equation is valid only for small p.

The dielectric properties of the spherical erythrocyte can be described by the single-shell model [2,16]. In the single-shell model the cell is considered as a conducting homogeneous sphere (or ellipsoid) covered with a thin shell, much less conductive than the sphere itself [2,3,16–19].

The effective dielectric permittivity of the cell is given by the equation:

$$\epsilon_c(\omega) = \epsilon_m^*(\omega)\frac{2(1-\nu) + (1-2\nu)E(\omega)}{(2+\nu) + (1-\nu)E(\omega)} \quad (2)$$

where

$$\nu = (1 - d/R)^3,\ E(\omega) = \frac{\epsilon_i^*(\omega)}{\epsilon_m^*(\omega)},$$

d is a thickness of membrane, R is the cell radius;

$$\epsilon_i^*(\omega) = \epsilon_i - i\frac{\sigma_i}{\epsilon_0 \omega},\ \epsilon_m^*(\omega) = \epsilon_m - i\frac{\sigma_m}{\epsilon_0 \omega},$$

with ϵ_i and ϵ_m being the particle interior and membrane static permittivities, σ_i and σ_m are their conductivities.

3. Materials and methods

3.1. Cell preparations

3.1.1. Red blood cells (RBC)

Fresh samples of human blood cells obtained from the Hadassah University Hospital blood bank were centrifuged for 5 min at $300 \times g$. The plasma and buffy coats were removed by careful aspiration. The red blood cells were then washed twice in phosphate-buffered saline (PBS), centrifuged and resuspended in diluted PBS solution (63–65%) and kept for few minutes, until they became spherical. They were then washed twice and resuspended in isotonic sucrose solution (ISP7.4 = 9 g sucrose in 100 g solution, including 5 mM sodium phosphate at pH 7.4). This procedure was needed in order to keep the cells in low conductive medium, in spherical shape. Cell suspensions were diluted by ISP7.4 for a given volume fraction.

3.1.2. Ghosts

Impermeable ghosts were prepared following the methods of Steck and Kant [20]. The first step is as above, in preparing the spherical RBC. The hemolysis was initiated by mixing 1 ml of packed cells with 50 ml of cold solution of 5p8 (5 mM sodium phosphate at pH 8.0). The membranous ghosts were pelleted at $22\,000 \times g_{max}$ for 10 min and washed twice in 5p8-1Mg (5 mM sodium phosphate at pH 8 + 1 mM $MgSO_4$) which caused them immediately to be sealed. Then the ghosts were washed twice in ISP7.4 and resuspended in the same medium to the desired volume fraction.

Volume fraction was measured in heparinized glass capillary tubes which were centrifuged for 5 min in a Clay Adams centrifuge. The reading of volume fraction was done with the aid of the built-in magnifying glass. For each measured cell suspension, a sample was taken and centrifuged to obtain the supernatant for the dielectric measurements.

3.2. Dielectric measurements and permittivity calculation

The general principles of Time Domain Dielectric Spectroscopy and a detailed description of the set-up used in our measurements has been described elsewhere [7–9,21,22]. A brief review of the method is given in Appendix A.

The set-up [22,25] consists of the Dipole TDS LTD (Jerusalem, Israel) time domain measuring system with a two-channel sampler, a step generator, a thermostabilized sampling head, a digital acquisition system (DAS), and a computer, PC AT 486/66. (The temperature can be computer-controlled in our set-up over the interval of $-30 \div +120$°C). The set-up utilized the difference method of measurement, with a unique registration of primary signals in a non-uniform time scale. This system permits five orders of frequency (10^5–10^{10} Hz) to be covered by one

single measurement. The results could be presented both in frequency (in terms of complex dielectric permittivity $\epsilon^*(\omega)$) and in time (in terms of the dielectric response function $\varphi(t)$) domains. The whole procedure of measurement and data treatment is carried out automatically.

The cell suspensions were measured in the total time-window of 5 μs. The minimum time step was 0.01 ns. Thus, the spectra were obtained in frequencies ranging from 200 kHz up to 2 GHz . A sample cell with golden electrodes with capacitance 0.065 pF was used. The temperature in the sample cell was controlled by a 'Heto' thermostat.

3.3. Experimental data treatment

The electrode polarization effect was taken into account by the method described in Appendix A. It was shown that the used volume fraction was small enough, so that the effective permittivity spectra of a single cell could be calculated according to the Maxwell mixture formula (Eq. 1). The obtained spectra, were fitted to the single-shell model (Eq. 2), and different structural and geometric parameters of erythrocytes and ghosts were estimated. Because of the complexity of these equations and large number of local minima the fitting by regular steepest descent method was impossible. Therefore the fittings were made by the Simulated Annealing method, described in Appendix B.

4. Results and discussion

4.1. Electrode polarization

The method of electrode polarization correction is presented in Appendix A. The method is applicable only to cell suspensions of small volume fractions (less then 10%) and relatively low conductivities (< 1 S/m). Fig. 1 shows the real part of the dielectric permittivity spectrum of the supernatant, obtained from the 7% erythrocyte suspension measured at room temperature. The expected dielectric permittivity of this solution does not depend on the frequency, and equals to 78, which is typical to the aqueous solutions of low molecular compounds. The frequency dependence of the dielectric permittivity appears due to the electrode polarization effect. The effect is more significant at low frequencies, but negligibly small at the frequencies above 1 GHz. As one can see, the effect of the electrode polarization can not be described by simple Debye process. So the effect is more complicated and could be fitted by Cole-Cole formula. The fitting results are given in Table 1.

Table 1
The parameters, describe the electrode polarization effect of the supernatant, obtained from the 7% erythrocyte suspension, calculated from the fitting to Cole-Cole equation

ϵ_s	ϵ_∞	τ (ns)	α
197	78	427	0.96

Fig. 2 represents the Cole-Cole plot of the complex dielectric permittivity spectrum of 7% erythrocyte suspension before taking into account the electrode polarization effect (1) and after (2). As one can see, the dielectric relaxation of the erythrocyte suspension before correction of the electrode polarization is described by Cole-Cole equation, as well as the pure electrode polarization effect. However, after the latter effect has been accounted for, the dielectric relaxation of erythrocyte suspensions is described by a simple Debye equation, which is in good agreement with the results, obtained by the frequency-domain methods [17–19,23,24]. The fitting results are represented in Table 2.

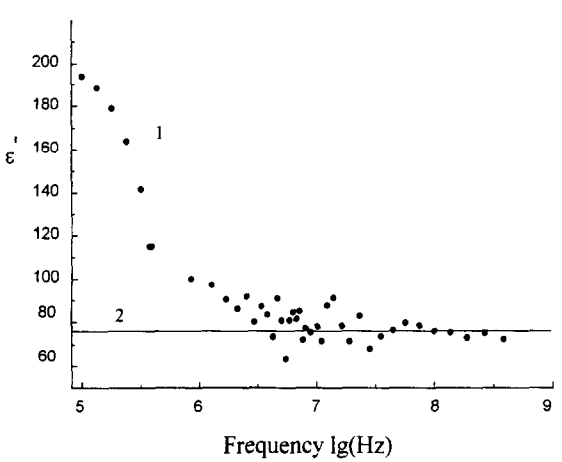

Fig. 1. (1) Real part of the dielectric permittivity spectrum of the supernatant, obtained from the 7% erythrocyte suspension; (2) its expected dielectric permittivity.

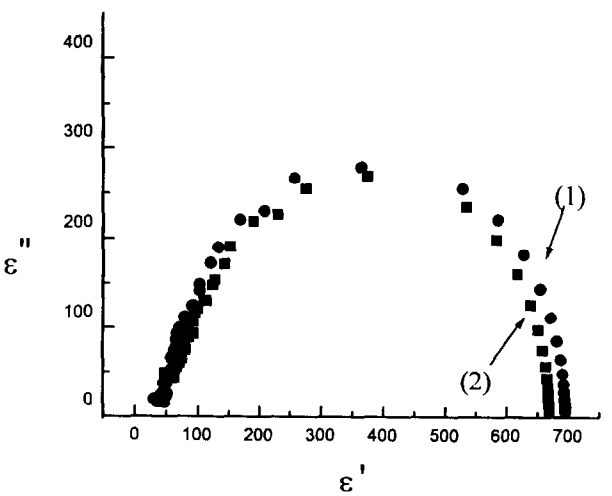

Fig. 2. Cole-Cole plot of the dielectric permittivity spectrum of 7% erythrocyte suspension. (1) Before taking into account the electrode polarization effect, (2) after it.

Table 2
The parameters, describing the dielectric relaxation of the 7% erythrocyte suspension, calculated from the fitting to Cole-Cole equation

Sample	ϵ_s	ϵ_∞	τ(ns)	α
1	700	78	254	0.98
2	670	77	261	1

(1) Before taking into account the electrode polarization effect, (2) after it.

All further results are given after correction of the electrode polarization.

4.2. Volume fraction dependence

The dielectric permittivity of cell suspension at each frequency is a function of the cells volume fraction. Fig. 3 shows the dielectric permittivity spectra of erythrocyte suspensions with four different cell volume fractions.

Fig. 4 shows the values of the real part of the dielectric permittivity corresponding to the frequency 5 MHz as a function of the cells volume fraction. It is seen that in the region of concentrations up to 20% the dielectric permittivity is a linear function of the volume fraction. It means that since the volume fraction is less than 20%, the cells in the suspension do not interact with each other, and the Maxwell mixture equation (Eq. 1) can be applied to the suspension. For the volume fractions larger then 20% the Hanai formula [16–18] has to be used.

Thus, it was shown that

(1) The electrode polarization effect can be taken into account by additional measurements of the corresponding supernatant.

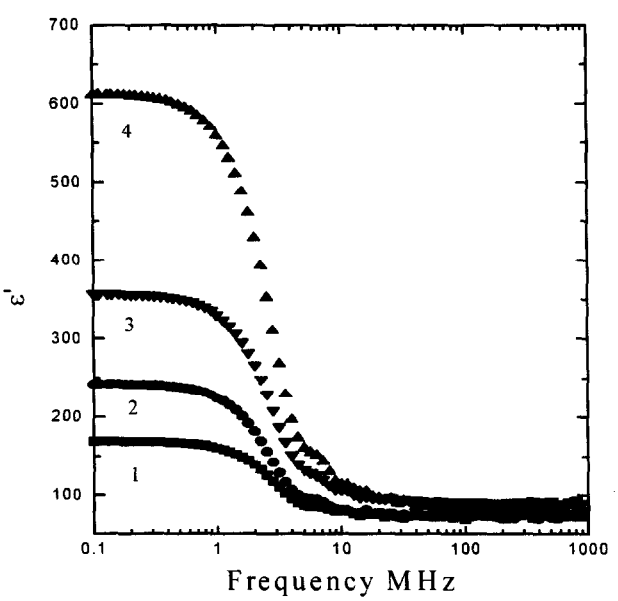

Fig. 3. Real part of the dielectric permittivity spectra of erythrocyte suspensions. 1–4% volume fraction, 2–9%, 3–11%, 4–26.5%.

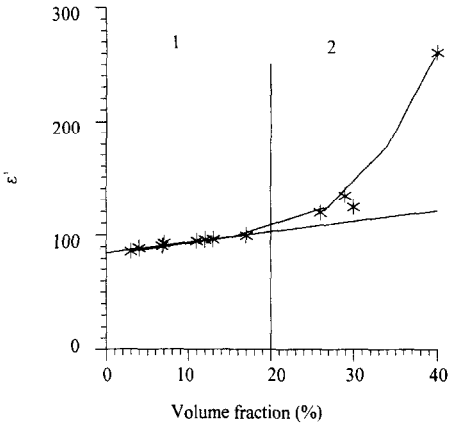

Fig. 4. Real part of the dielectric permittivity, corresponding to frequency the 5 MHz as a function of the cells volume fraction. (1) The concentration region, where the permittivity is a linear function of concentration. (2) The concentration region, where the permittivity is non-linear function of concentration.

(2) The optimal cell concentration for TDDS measurements varies from 3% to 20%. The low limit is due to the set-up sensitivity, the upper one is due to the model application limitations, i.e., for cell concentrations greater then 20% the intercellular interactions become significant.

4.3. Erythrocytes and ghosts

The erythrocyte and erythrocyte ghost suspensions are very similar systems. They differ in their inner solution (in the case of erythrocytes it is an ionic haemoglobin solution; in the case of ghosts it is almost like the surrounding solution in which they were while they were sealed). Cell sizes in prepared suspensions depend on the ion concentration in the supernatant and in the cell interior. Thus the dielectric spectra of erythrocytes and ghosts suspensions have the same shape, which means that there are no additional (except Maxwell-Wagner) relaxation processes in the erythrocyte cytoplasm, and single-shell model (Eq. 2) can be applied.

The frequency dependence of the effective dielectric permittivity of a single average erythrocyte was calculated according to (Eq. 1). The dielectric permittivity spectrum of a single 'average' erythrocyte is shown in Fig. 5 by points. The relaxation process of the single erythrocyte can be described by the Debye equation. The effective dielectric permittivity spectra of an 'average' erythrocyte were fitted to the single-shell model equation (Eq. 2), and the phase parameters of the cell were found. The fitted dielectric spectrum is given in Fig. 5 by a solid line.

The membrane dielectric permittivity ϵ_m was evaluated from fitting with the accuracy ± 0.05 (see Appendix B), the membrane conductivity cannot be estimated from the fitting as far as it is less then the accuracy within which it can be calculated, so it must be set to zero. Insufficient accuracy of the inner phase dielectric permittivity ϵ_s al-

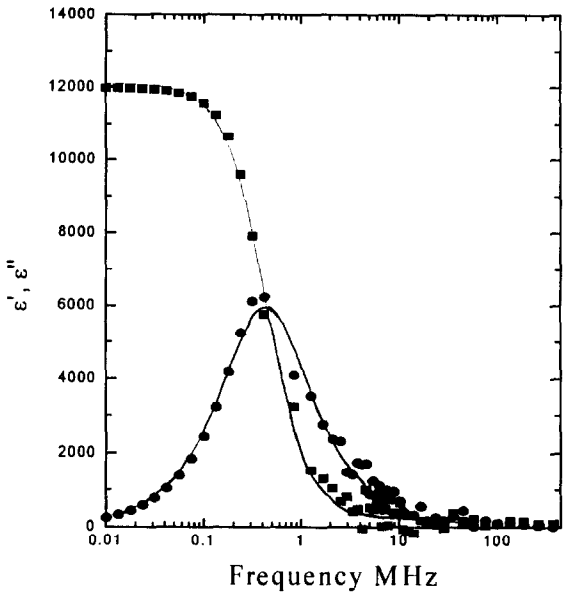

Fig. 5. The dielectric permittivity spectrum of the 'average' erythrocyte fitted to the single-shell model. The experimental results are figured by points, the fitting results by a solid line.

lows only to estimate the lower and upper limits of its value. The inner phase conductivity σ_i was found with accuracy of ± 0.001 S/m. The dimensionless parameter v was found with the accuracy of $\pm 1 \cdot 10^{-4}$.

As regards the ghosts, their membrane dielectric permittivity ϵ_m is that of the erythrocytes they were prepared from. The inner phase conductivity σ_i of ghosts varied in correspondence with the conductivity of the supernatant they were placed in. Parameter v depends on the supernatant conductivity and on the method of the ghosts preparation.

The limits of phase parameters variation of different erythrocytes and ghosts at room temperature are given in Table 3. The membrane dielectric permittivities of erythrocytes was found to be distributed near 5. The distribution is shown on Fig. 6. The membrane thickness of erythrocyte was found to be 3.1 nm assuming the average effective radius is 2.7 μm. This result is in a good agreement with that obtained by Fricke [13,14].

Thus, it was shown that one can apply the mixture equation (Eq. 1) and single-shell model (Eq. 2) to dilute solutions of ghosts and erythrocytes. The membrane dielectric permittivity, cytoplasm conductivity and geometric parameter ν for each kind of cells were calculated. The

Table 3
The limits of phase parameters variation of different erythrocytes and ghosts at room temperature

Sample	ϵ_m	$v\left(1-\frac{d}{R}\right)^3$	d (nm) independent measurement $R = 2.7$ μm
Erythrocytes	~ 5	~ 0.9967	~ 3.1
Ghosts	~ 4.8	~ 0.9967	~ 3.1

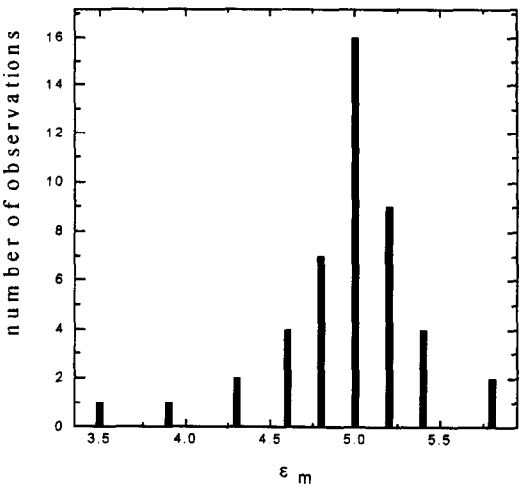

Fig. 6. The distribution of the observed values of the membrane dielectric permittivity.

accuracy of the lumped capacitance method is, however, insufficient for the evaluation of the cytoplasm dielectric permittivity and the membrane conductivity, and another approach to estimate it is needed.

Acknowledgements

We would like to thank Mrs. Rivka Hadar for her excellent technical assistance in preparing the various cell suspensions.

Appendix A. Electrode polarization correction and main principles of TDDS

The technique used in this work is called lumped capacitance method [22]. In this method the sample cell may be treated like a capacitor with capacitance $\epsilon^* C_0$ where ϵ^* is the sample permittivity and C_0 is the capacitance of the empty capacitor, which can be calculated from its geometric parameters.

The expression for the complex dielectric permittivity of the sample in the frame of this method [22,25] is:

$$\epsilon^*(\omega) = \frac{1}{i\omega C_0}\frac{I_Q(\omega)}{V(\omega)} \qquad \text{(A1)}$$

where $I_Q(\omega)$ is the Fourier image of the current which flow through the capacitor and $V(\omega)$ is the Fourier image of voltage on it.

If the measured solutions have high conductivity, a problem arises due to the formation of a layer of ions near the electrodes [1,10–12]. This modifies the field distribution within the test liquid. The phenomenon is known as the electrode polarization effect. The electrode polarization effect can be taken into account by change of the equivalent circuit of the sample cell. The layer of ions near the

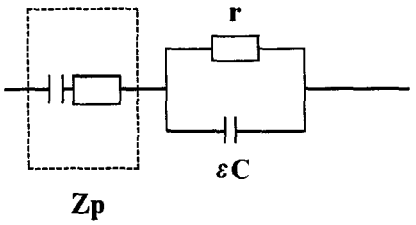

Scheme 1. The equivalent circuit accounting for the electrode polarization.

electrodes can be considered like some capacitor and resistance inserted in series with the capacitor filled with the sample [1,2,10–12] (see Scheme 1). These capacitance and resistance can be considered like some complex impedance Z^p.

Thus, the following relation for the unknown impedance can be written in frequency domain:

$$Z_X(\omega) = Z_0 \frac{v_0(\omega) - r_X(\omega)}{v_0(\omega) + r_X(\omega)} = Z_X^p(\omega) + \frac{R_X}{1 + i\omega\epsilon_X^*(\omega) C_0 R_X} \quad \text{(A2)}$$

where $v_0(\omega)$ and $r_X(\omega)$ are the Fourier transforms of the incident and reflection signals $V_0(t)$ and $R_X(t)$, respectively. A similar relationship can be written for the reference sample (a supernatant):

$$Z_s(\omega) = Z_0 \frac{v_0(\omega) - r_s(\omega)}{v_0(\omega) + r_s(\omega)} = Z_s^p(\omega) + \frac{R_s}{1 + i\omega\epsilon_s C_0 R_s} \quad \text{(A3)}$$

The above relationship must meet the following requirements: $R_x = R_s = R$, $Z_s^p = Z_x^p = Z^p$ and $\epsilon_s^*(\omega) = \epsilon_s =$ const. The combination of Eq. (A2) and Eq. (A3) provides the basic formula for electrode polarization correction:

$$\epsilon_x^*(\omega) = \frac{\epsilon_s - \dfrac{A(\omega)}{i\omega C_0 R} - A(\omega)\epsilon_s}{A(\omega) + i\omega A \epsilon_s C_0 R + 1} \quad \text{(A4)}$$

where $A(\omega) = (Z_X(\omega) - Z_s(\omega))/R$, and R is the sample resistance. It was found that the effect of electrode polarization is the same for both cell suspensions with small volume fractions (less than 15%) and their supernatants. So, Z^p must therefore be calculated from the additional measurement of the supernatant, which has the same conductivity as the cell suspension, and its dielectric permittivity is known from high frequency measurements.

Appendix B. Fitting by the simulated annealing method

The Simulated Annealing method is a modification of the Temperature Algorithm of Metropolis (realization of Monte-Karlo) of numerical simulations. The method consists of the following procedure: suppose we have some function $F(a_i)$ of p parameters $a_i (i = 1,p)$, which has to be minimized in the space of parameters a_i. First, some reasonable guess about the initial values of parameters is made, and each of the parameters is given its increment $\Delta a_i > 0$. At each calculation step one chooses at random which of the parameters a_i is to be updated. Next, it is randomly chosen whether the parameter will be updated in positive ($a_i(k+1) - a_i(k) = \Delta a_i$ or in negative ($a_i(k+1) - a_i(k) = -\Delta a_1$) direction ($k$ is a number of the step). The corresponding function change would be $\Delta F = F(k+1) - F(k)$. After that, the decision has to be made whether to accept the new (updated) value of the parameter a_i. If $\Delta F < 0$ the positive decision (to accept the new value) is taken with the probability 1, whereas in case $\Delta F > 0$ the positive decision is taken with the probability $\exp(-\Delta F/T)$, where T is numerical 'temperature', which has to be also chosen in the optimal way in order to avoid local minima. As the function approaches the global minima, the temperature and the parameters increments Δa_i have to be made smaller and smaller, until the desired accuracy is achieved.

The particular way of updating Δa_i and T depends on the specific problem and requires delicate treatment. In principle the described algorithm allows one to perform the minimization of any complicated function with large number of local minima, provided there has been made a right choice of the temperature and the parameters increments values.

In our case the sum of squares of the deviations of the experimentally found dielectric permittivity from its theoretical values (calculated from either of the models) over all experimental frequencies stands for the function $F(a_i)$, to be minimized.

$$F(a)_i = \sum_n \left[(\epsilon'_n - \epsilon'_{\text{model}}(\omega_n, a_i))^2 + (\epsilon''_n - \epsilon''_{\text{model}}(\omega_n, a_i))^2 \right] \quad \text{(B.1)}$$

where ϵ'_n, ϵ''_n are the experimental values of real and imaginary parts of the dielectric permittivity for the frequency ω_n, respectively and $\epsilon'_{\text{model}}(\omega_n, a_i)$, $\epsilon''_{\text{model}}(\omega_n, a_i)$ are their respective theoretical values.

The temperature is chosen at each step to be proportional to the derivative of the function F with respect to the parameter a_i chosen for updating.

Accuracy of fitting of each parameter can be estimated from the formula:

$$\Delta a_i = \Delta F \Big/ \frac{\partial F}{\partial a_i}$$

where ΔF and $(\partial F/\partial a_i)$ are calculated with parameters a_i found from fitting.

References

[1] Grant, E.H., Sheppard, R.J. and South, G.P. (1978) Dielectric Behavior of Biological Molecules in Solution, Clarendon, Oxford.
[2] Takashima, S. (1989) Electrical Properties of Biopolymers and Membranes, IOP Publishing.
[3] Bone, S. and Zaba, B.(1992) Bioelectronics, John Wiley & Sons.
[4] Pethig, R. and Kell, D.B. (1987) Phys. Med. Biol. 32, 933–970.
[5] Bordi, F. Cametti, C. and Di Biasio, A. (1990) Biochim. Biophys. Acta 1028, 201–204.
[6] Harris, C.M., Todd, R.W., Bungard, S.J., Lovit, R.W., Morris, J.G. and Kell, D.B. (1987) Enz. Micr. Technol. 9,181–186.
[7] Feldman, Yu.D., Zuev, Yu.F., Polygalov, E.A. and Fedotov, V.D. (1992) Colloid Polymer Sci. 270, 768–780.
[8] Cole, R.H., Berberian, J.G., Mashimo, S., Chryssik, G., Burns, A. and Tombari, E. (1989) J. Appl. Phys. 66, 793–802.
[9] Bone, S. (1988) Biochim. Biophys. Acta 967, 401–407.
[10] Schwan, H.P. (1992) Ann. Biomed. Eng. 20, 269–288.
[11] Davey, C.I., Markx, G.H. and Kell, D.B. (1990) Eur. Biophys. J. 18, 255–265.
[12] Schwan, H.P and Ferris, C.D. (1968) Rev. Sci. Instrum. 39, 481–485.
[13] Fricke, H. (1953) Nature 4381, 731–732.
[14] Fricke, H. (1953) J. Phys. Chem. 57, 934–937.
[15] Garsia, A., Grosse, C. and Brito, P.J. (1985) Phys. D. Appl. Phys. 18, 739–745.
[16] Hanai, T., Asami, K. and Koizumi, N. (1979) Bull. Inst. Chem. Res. Kyoto Univ. 57, 297–305.
[17] Asami, K., Hanai, T. and Koizumi, N. (1980) Jpn. J. Appl. Phys. 19, 359–365.
[18] Asami, K. Takahashi, Y. and Takashima, S. (1989) Biochim. Biophys. Acta 1010, 49–55.
[19] Asami, K. and Irimajiri, A. (1984) Biochim. Biophys. Acta 778, 570–578.
[20] Steck, T.L. and Kant, J.A. (1974) Biomembranes 31, 172–180.
[21] Cole, R.H. and Winsor, P. IV (1982) Time Domain Dielectric Spectroscopy. Fourier, Hadamard, and Hilbert transforms in chemistry (Marshall, A.G., ed.), Plenum Press, New York.
[22] Ermolina, I.V., Polygalov, E.A., Romanychev, G.D., Zuev, Yu.F. and Feldman, Yu.D. (1991) Rev. Sci. Instrum. 62, 2262–2265.
[23] Bone, S., Ginzburg, B.Z., Morgan, H., Wilson, G. and Zaba, B. (1993) Phys. Med. Biol. 38, 511–520.
[24] Bevig, H., Eriksson, L.E.G., Davey, C.L. and Kell, D.B. (1994) Eur. Biophys. J. 23, 207–218.
[25] Feldman, Y., Andrianov, A., Polygalov, E., Romanychev, G., Ermolina, I. and Zuev, Y. (1995) Rev. Sci. Instrum., in press.